ISTITUTO NAZIONALE DI FISICA NUCLEARE
Laboratori Nazionali di Frascati

LNF-81/21

J. Duflo, J. Berger, L. Goldzahl, J. Oostens, F. L. Fabbri, P. Picozza, L. Satta, G. Bizard, F. Lefebrevs, J. C. Steckmeyer and D. Legrand:
STUDY OF THE INCLUSIVE INELASTIC REACTION $\alpha+\alpha \rightarrow \alpha+X$ AT 4.32 GeV/c AND 5.07 GeV/c IN THE FORWARD DIRECTION

Estratto da:
Nuclear Physics A356, 427 (1981)

Servizio Documentazione
dei Laboratori Nazionali di Frascati

Nuclear Physics **A356** (1981) 427–444

STUDY OF THE INCLUSIVE INELASTIC REACTION $\alpha+\alpha\rightarrow\alpha+X$ AT 4.32 GeV/c AND 5.07 GeV/c IN THE FORWARD DIRECTION

J. DUFLO, J. BERGER, L. GOLDZAHL and J. OOSTENS*

Institut National de Physique Nucléaire et de Physique des Particules, Laboratoire National Saturne, Saclay, France

F.L. FABBRI, P. PICOZZA and L. SATTA

Istituto Nazionale di Fisica Nucleare, Laboratori Nazionali di Frascati, Frascati, Italy

G. BIZARD, F. LEFEBVRES and J.C. STECKMEYER

Laboratoire de Physique Corpusculaire, LA34 associé à l'IN2P3, ISMRA, Université de Caen, Caen, France

and

D. LEGRAND

Département de Physique Nucléaire, Centre d'Etudes Nucléaires de Saclay, Saclay, France

Received 28 May 1980
Revised 9 October 1980

Abstract: The reaction $\alpha+\alpha\rightarrow\alpha+X$ was measured between 3° and 11° in the laboratory, at 4.32 GeV/c and 5.07 GeV/c incident momenta. The spectra are described as an incoherent sum of quasielastic scattering on substructures of the α-target. These quasielastic cross sections have a diffractive form comparable to that of the known elastic scattering process. They are reproduced by Glauber-model calculations which use radii for these substructures much smaller than those of the free nuclei.

E

NUCLEAR REACTION ^{4}He(α, α)X, P = 4.32, 5.07 GeV/c; T = 0.495 GeV/N, 0.641 GeV/N; measured σ(p, θ); extracted $\sigma(\bar{t})$ for quasielastic scattering on α-substructures; comparison with multiple scattering models.

1. Introduction

Using the synchrotron Saturne I at Saclay, the inclusive reaction

$$\alpha+\alpha\rightarrow\alpha+X \tag{1}$$

was measured at 4.32 GeV/c and 5.07 GeV/c incident momenta for values of the four-momentum transfer, t, lying between 0.05 (GeV/c)^2 and 0.8 (GeV/c)^2. These data were taken at the same time as our measurements of $\alpha\alpha$ forward-angle elastic scattering at the same energies [1]).

* Present address: Physics Department, University of California at Los Angeles, Los Angeles, CA 90024, USA.

In this energy region we have observed that the Glauber theory can account fairly well for the $\alpha\alpha$ elastic scattering process up to values of $t \approx 0.5$ (GeV/c)^2 [ref. [1])]. We are also interested in determining whether this theory can account for the present inelastic results. We present here an analysis of this inclusive reaction data in terms of quasielastic scattering on clusters in the α-target. In this study the α has the advantage of being a light and relatively simple nucleus, since its wave function at low momentum transfer can be correctly represented by a harmonic oscillator wave function. Due to the small number of nucleons, it is possible to study its clusters which, if they exist, will not be numerous and so more easily discernible. It should also be noted that the interpretation is made easier by the fact that the α has spin and isospin zero. Also, since we are in the intermediate energy range ($T = 0.495$ GeV/N and 0.641 GeV/N), reaction (1) is less affected by absorption and distortion in the entrance and exit channels [2,3]) than at low energy, especially in the case of the detected α whose momentum is close to that of the incident α's. It is possibly more interesting to study this reaction by observing the emitted fragments rather than the scattered α, but the fragments are emitted over the full solid angle and most frequently with small momenta. From a purely experimental point of view, their detection is more difficult. In particular for the low-t processes studied in this work the velocities of the emitted fragments are relatively close to typical nuclear velocities, so final-state interactions are very important, distorting the picture of the nucleus that could be extracted. It is obvious that a coincidence experiment that would detect both the scattered α and the fragments would give the most complete information.

2. Description of the experiment

The present experiment used the α-beam extracted from the synchrotron Saturne I at Saclay. This beam of 2×10^{10} α-particles per cycle is focussed as a 1 cm high by 2 cm wide spot on a 5.6 cm long helium target. The scattered particles were analysed by an achromatic double focussing spectrometer with a solid angle of 0.11 msr defined by a lead collimator 4×8 cm. A detailed description of this layout has already been published [4]). The horizontal angular acceptance of the spectrometer is ± 3.8 mrad, and there is a ± 2 mrad uncertainty on the central scattering angle. The momenta are measured at an intermediate focus by a five counter hodoscope covering a band of relative momentum $\Delta P/P = 5\%$ with a momentum resolution of 1.05% (FWHM). The scattered α's were identified by their time of flight over a 14 m path and by their energy loss in the hodoscope and in the set of three scintillation counters at the final focus. Deuteron contamination is small ($< 2\%$). The incident beam was monitored by two-counters telescopes: one aimed at a thin foil located upstream of the helium target, the other directed at the helium target. The stability of the two monitors is reliable to $\approx 1\%$. At both incident momenta absolute flux calibration was obtained by measuring the activity induced in a graphite disc by the

reaction $^{12}C(\alpha, X)^{11}C$, whose cross section has been measured in the same momentum region [5]).

3. Results

3.1. $(d^2\sigma/d\Omega\, dp)_{lab}$ SPECTRA

At 4.32 GeV/c ($T = 0.495$ GeV/N) we measured 14 spectra between 3° and 11° in the laboratory. At 5.07 GeV/c ($T = 0.641$ GeV/N) we measured 13 spectra between 3° and 10°. The data were corrected for the empty-target background ($\leq 20\%$) and for nuclear absorption ($\leq 10\%$).

The set of $d^2\sigma/d\Omega dp$ inclusive spectra is presented in fig. 1. The errors shown are statistical. There is also a systematic error of 10% resulting from the measurement of beam intensity and from determining the solid angle of the spectrometer. The spectra were measured over a momentum band of about 200 to 300 MeV/c.

3.2. $d\sigma/d^2q$ INTEGRATED SPECTRA

Integration of the inelastic spectra on the momentum of the scattered α's gives the inclusive inelastic cross section $d\sigma/d\Omega_{lab}$ of the reaction $\alpha + \alpha \rightarrow \alpha + X$ in the region analysed. The $d\sigma/d^2q$ cross sections resulting from these integrations are shown in fig. 2, q being the average transverse momentum of the spectrum measured. For the largest angles studied ($q \geq 0.55$ GeV/c) where the spectra were not measured over a sufficiently large momentum range, we have included an estimate of the lower limit of the integration, taking into account the resolution of the spectrometer. For these angles, we have also included an estimate of the cross section deduced from the analysis explained later. Also, in fig. 2, we have included the differential cross section $d\sigma/d^2q$ for the $\alpha\alpha$ elastic scattering [1]). The comparison of these cross sections illustrates the rapid relative variation of the elastic and inelastic parts of the spectra presented in fig. 1. It can be seen that the inelastic cross section dominates beyond $q = 0.5$ GeV/c. Two striking features of this inclusive inelastic cross section should be noted: it is independent of the incident energy in the range measured; and it shows a clear diffraction structure around $q = 0.45$ GeV/c.

4. Global interpretation of the inelastic spectra

Using the Glauber and Matthiae [6]) multiple scattering model, Fujita and Hüfner [7]) calculated the hadron–nucleus inclusive cross section and have compared it with our preliminary results [8]) for $\alpha\alpha$ at 4.32 GeV/c. In this calculation no free parameters are used, the α-projectile is considered to be an elementary particle; and the $d\sigma/d^2q$ cross section is expressed as a function of αp, elastic scattering measured at 7 GeV/c [ref. [9])] and approximated by a gaussian, $\exp(-q^2/p_0^2)$, with $p_0 = 185$ MeV/c. The

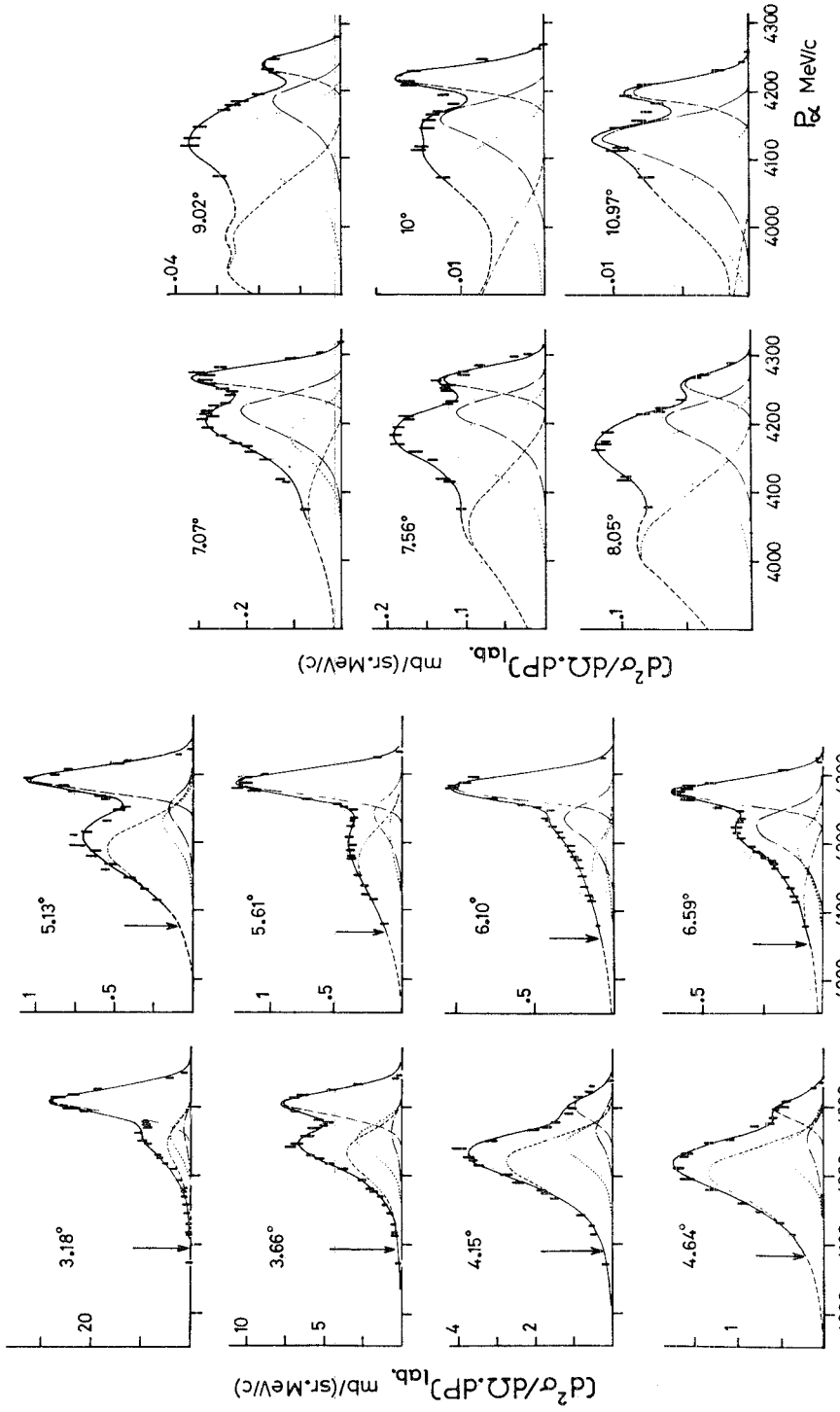

Fig. 1a. Inclusive cross sections $(d^2\sigma/d\Omega\, dp)_{lab}$ for the reaction $\alpha + \alpha \rightarrow \alpha + X$, at 4.32 GeV/$c$ incident momentum. The inelastic part of the spectra has been analysed as the sum of quasielastic scatterings. The curves are as follows: long dashes represent the elastic peak corresponding to the spectrometer resolution; short-dashed, dotted, and dot-dashed lines correspond to quasielastic scattering on the substructures N, d and ^{3}He/^{3}H; the solid line is for the sum of these contributions. The arrows indicate the threshold of the π-production.

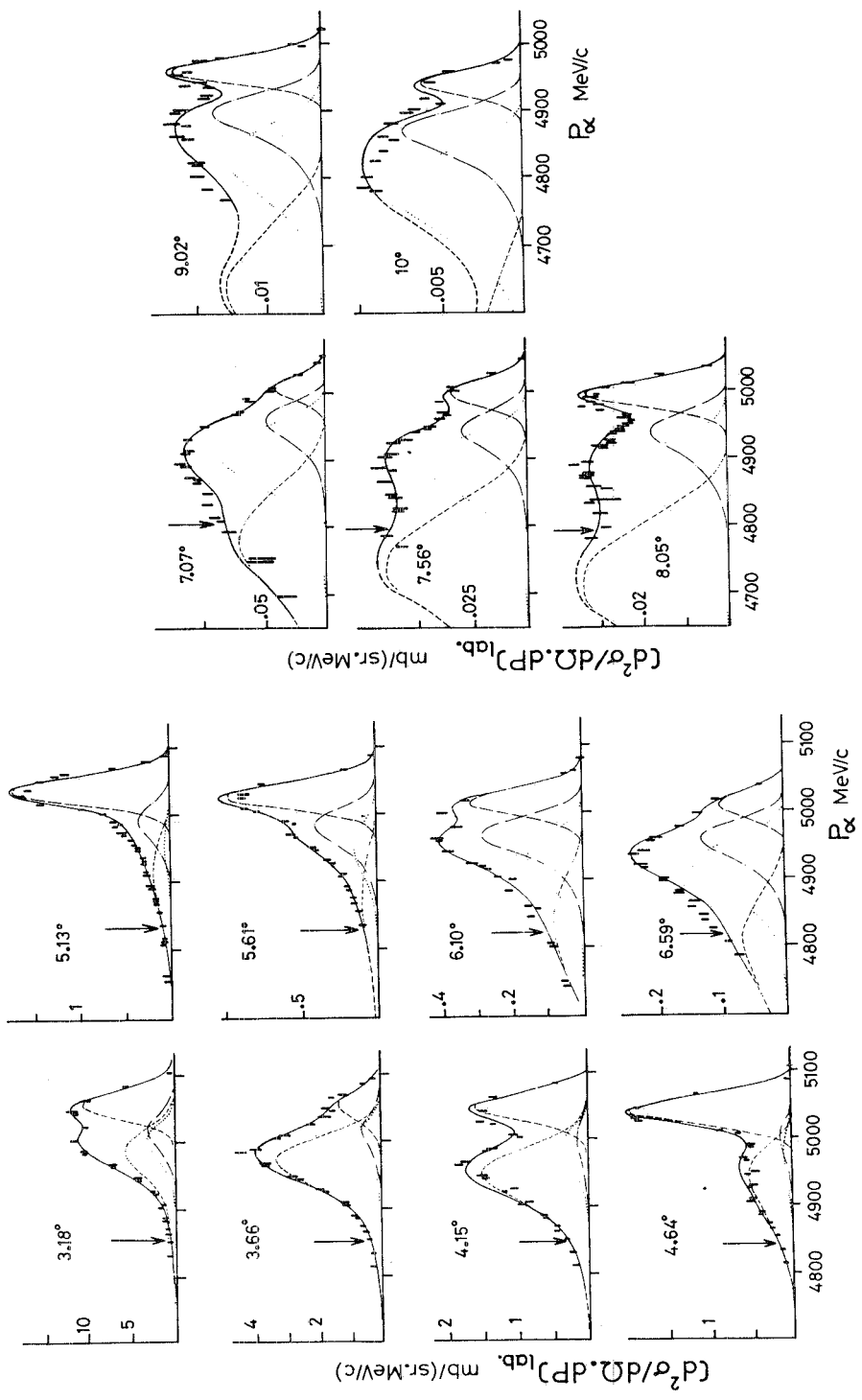

Fig. 1b. The same as fig. 1a, at 5.07 GeV/c incident momentum.

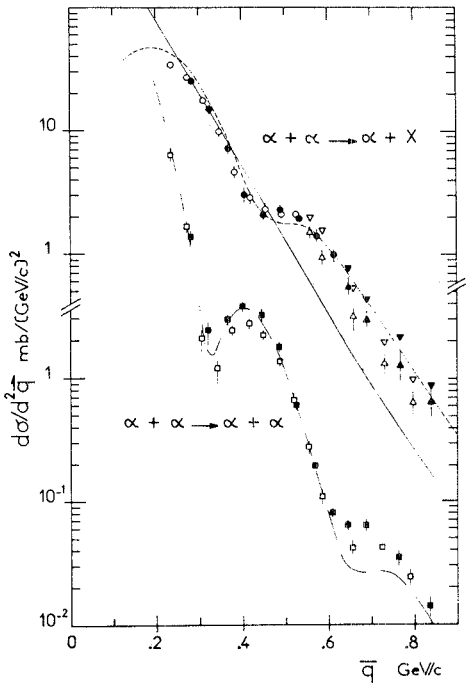

Fig. 2. Inclusive inelastic cross sections $d\sigma/d^2q$ at 4.32 GeV/c and 5.07 GeV/c, q being the transverse momentum. The symbols are as follows: ○ and ●: integrated spectra of the figs. 1a and 1b without the elastic peak; △ and ▲: estimates of the lower limit of the integration for the incomplete spectra at large angles and ▽ and ▼: estimates for these incomplete spectra based on the cross sections calculated by the quasielastic scattering analysis; the solid line is the result of the Fujita and Hüfner [7]) calculations; □ and ■: $\alpha\alpha$ elastic cross sections at 4.32 GeV/c and 5.07 GeV/c; the dot-dashed line represents the calculations based on the Czyz and Maximon model [33]) for $\alpha\alpha$ elastic scattering at 5.07 GeV/c, with the same NN interaction parameters used in ref. [1]); i.e., scattering amplitude Re/Im ratio $\alpha = -0.37$, elastic scattering slope $\beta = 2.75$ (GeV/c)$^{-2}$ and total cross section $\sigma = 39.5$ mb.

results of this calculation for the inclusive spectra are shown as a solid line in fig. 2. This calculation reproduces the order of magnitude and the slope of the inclusive cross section but fails to reproduce the diffractive structure observed. This failure is perhaps due to the fact that in this calculation, neither the non-elementary aspect of the projectile, nor the diffractive behaviour of the αp scattering process [10]) is taken into account. Lastly, in fig. 2, we show the result of the analysis of the inclusive data in terms of quasielastic scattering on clusters as a dotted line. This analysis will be discussed in detail in sects. 5 and 6.

5. Analysis of the inelastic spectra

5.1. THE VARIOUS POSSIBLE CONTRIBUTIONS

Various reactions can contribute to the spectra measured, and no one contribution can be excluded *a priori*:

In general, the region measured lies below the production threshold of the pion. However, for many angles, we studied the region where pion production is possible. In figs 1 the arrows indicate the threshold of the reaction $\alpha\alpha \rightarrow \alpha p^3H\pi^\circ$. No particular effect is noted in this region.

In the study of the $\alpha\alpha$ elastic scattering [1]) we looked at possible contributions from the excitation of the first excited state of ^{4}He (20.2 MeV)[ref. [11])]. Other levels could contribute to the inelastic bump as has been shown in particular by Haase *et al.* [12]) in the study of the ^{4}He(α, α')d, in kinematic conditions that favour the interaction in the final state and, as Bevelacqua has predicted [13]), up to 80 MeV. However, these authors do not provide information about the importance of these contributions.

Lastly, the collective phenomena reported by Frascaria *et al.* [14]) at around 50 MeV in the symmetric systems ^{40}Ca-^{40}Ca and ^{63}Cu-^{63}Cu are unlikely for the $\alpha\alpha$ system; the same is true for the giant resonances predicted by Liu and Brown [15]) for ^{16}O–^{16}O or heavier systems. In the absence of precise data about these two last contributions, we have ignored them in this analysis.

Looking carefully at the spectra represented in fig. 1 it will be noted that the inelastic bumps are centred at momenta which correspond to α-elastic scattering on "targets" of different masses. This is particularly noticeable in fig. 1a by comparing the spectra at 5.13° and at 6.59°, where the maximum of the bump appears at a higher momentum at 6.59° than at 5.13°, indicating the presence of at least two 2-body processes, each varying rapidly with angle. Since substantial probabilities for (p, ^{3}H), (n, ^{3}He) and (d, d) structures have been found in other experiments, we were prompted to analyse our results as a function of these configurations – [the two structures (p, ^{3}H) and (n, ^{3}He) that are kinematically indistinguishable in our experiment will be designated in this paper by (N, ^{3}He/^{3}H)]. The ^{4}He p $\rightarrow$ ^{3}He n p break-up reaction with ^{3}He or n as spectator that was observed by Glagolev *et al.* [16]) can be quoted as an example as can the α-fragmentation by hydrogen at 6.85 GeV/c studied by Berger *et al.* [4]). With these data, Bizard and Tekou [17]) using a Glauber model calculated that a 60% probability of (N, ^{3}He/^{3}H) was necessary to explain the results, provided that new particle production and final state interactions are ignored. The (d, d) configuration has already been put forward to interpret the experimental results, such as those of Wu *et al.* [18]). They apply the Serber model [19]) to their measurements of α-projectile fragmentation at $T = 140$ MeV in the heavy nucleus field (Ni, Zr, Bi, Th), where they observed an abundant production of deuterons. Also, at 156 MeV, Frascaria *et al.* [20]), from measurements of the ^{4}He(p, pp)^{3}H and ^{4}He(p, pd)d reactions, observed that the relative cross section of the deuteron is almost one sixth that of tritium. Finally, from a theoretical point of view, the (d, d) configuration of ^{4}He has been discussed by Lim [21]) based on a set of studies using various types of wave functions for ^{4}He. His conclusion is that the probability of this configuration is about 50%. This probability seems particularly high; but Lim [21]) stresses that "^{3}He-n, ^{3}H-p, and d-d descriptions of ^{4}He may not be orthogonal and in no sense does a large parentage for ^{3}He-n, ^{3}H-p clusters imply a small d-d overlap with ^{4}He".

In the absence of data for the (d, 2N) and (4N) configurations, and in spite of the fact that these states are conceivable, we have not taken them into account in our analysis. Double scattering on the two substructures, with subsequent fragmentation of the α, have been also overlooked. This rescattering effect can nevertheless become important at higher transfers, as has been noted by Azghirev *et al.* [23]) in $dd\rightarrow dX$ at 8.9 GeV/c and by Berger *et al.* [24,25]) in $\alpha d\rightarrow\alpha X$ at 3.98 GeV/c. Lastly, based on the calculations of Redish *et al.* [22]) for knock-out reactions produced by protons at energies of 300 MeV, we have assumed that off-shell effects are not significant for the α-particles at our energies.

5.2. DIFFERENTIAL CROSS SECTIONS FOR α-SCATTERING ON SUBSTRUCTURES OF THE TARGET

5.2.1. Calculation of the quasielastic spectra. In the analysis of our inelastic data we have retained only the (N, ^{3}He/^{3}H) and (d, d) configurations for the α-target, with the proportion of the configuration (X, X'), in which X and X' are the conjugate substructures, being treated as an adjustable parameter $\gamma_{XX'}$. Integration of each partial spectrum $S_{XX'}=(d^2\sigma/d\Omega dp_3)_{XX'}$ over the momentum p_3 of the scattered α, gives the contribution $C_{XX'}=\gamma_{XX'}(d\sigma/d\Omega)_{XX'}$ of the quasielastic scattering on the substructure X of the α-target, X' being a spectator. The observed spectra are interpreted as resulting from an incoherent sum $\Sigma C_{XX'}$ of the partial spectra. The shape of the spectra $S_{XX'}$ has been calculated in terms of the Fermi momenta of the substructures X and X' for each of the two incident momenta P_1 and for each angle θ_3 of the scattered α's studied. Each spectrum $S_{XX'}$ is constructed using the kinematics of the α-elastic scattering on X, with the following total energy and momentum:

$$E=E_i-E_{X'}, \tag{2}$$

$$\boldsymbol{P}=\boldsymbol{P}_1+\boldsymbol{P}_F, \tag{3}$$

where E_i is the total energy of the two α-particles before the reaction, $E_{X'}$ is the energy of the spectator X' having the Fermi momentum $-\boldsymbol{P}_F$ and $\boldsymbol{P}_1$ is the incident momentum of the α-projectile.

For each configuration (X, X') we used an isotropic momentum distribution $\Phi(p_F)$, such as:

$$\Phi(p_F)=|\phi(p_F)|^2\,p_F^2, \tag{4}$$

where $\phi(p_F)$ is the Fourier transform of the relative (X, X') wave function. For the (N, ^{3}He/^{3}H) configuration we used the Eckart parametrisation [26])

$$\psi(r)=N\frac{1}{r}\exp(-\alpha r)(1-\exp(-\beta r))^n, \tag{5}$$

where N is the normalisation constant, α is the separation energy decay constant, and β and n are real parameters which give good agreement with the results of

electron scattering on ^{4}He: $\alpha = 0.846\ \mathrm{fm}^{-1}$, $n = 4$, $\beta = 1.42\ \mathrm{fm}^{-1}$. For the (d, d) configuration we chose a gaussian representation for the wave function in momentum space:

$$\phi(p_t) = (\pi/p_0^2)^{1/2} \exp(-p_F^2/2p_0^2), \tag{6}$$

with $p_0 = 130\ \mathrm{MeV}/c$, a value which is compatible with the results of Frascaria *et al.* for the reaction ^{4}He(p, pd)d [ref. [20])]. This distribution can also be calculated using statistical models of fragmentation processes [27]) that are proposed for the fragmentation of heavy ions (^{12}C, ^{16}O) on different targets. Similar distributions have also been observed by Wu *et al.* [28]) in the fragmentation of α's at $T = 80$ and 160 MeV. Variations of $\pm 10\%$ on p_0 have been made in order to test the sensitivity to the adopted value for p_0. These variations caused no significant changes in our results.

In the construction of partial spectra $S_{XX'}$, account is taken of the fact that X is in motion. Since the mean value of the Fermi momentum of X is small compared with the incident momentum of the α-particle, this correction to the final partial spectrum is always weak and we found practically that the necessary iteration order in the calculation is equal to or less than three. A gaussian spread is introduced in the calculation to take into account the spectrometer resolution.

Finally, the absolute values of $C_{XX'}$ are evaluated by fitting the partial spectra to the observed spectra, using a χ^2 method.

5.2.2. Results of the fit and integrated cross sections. The results of the final adjustment of the calculated partial spectra to the measured spectra are shown in fig. 1. For both energies and for the whole set of angles the adjustment is generally in good agreement with the experimental data. For angles beyond 9° lab, where the measured spectra are incomplete, the quasielastic scattering contribution αN was normalised so as to follow the angular variation of αp scattering [29,30]).

For large angles, the separation between the $\alpha\alpha$ elastic peak and the α-^{3}He/^{3}H spectrum is less well reproduced by the calculation than for small angles. What is probably being seen is the effect of double scattering by the incident α on clusters in the target, whose possible contribution has already been mentioned. In fact, such a contribution, since it entails the participation of all the nucleons in the α-particle must be centred at a momentum close to that of the elastically scattered α to within the fragmentation energy, either 20 MeV for (N, ^{3}He/^{3}H) or 24 MeV for (d, d). This contribution is superimposed on the possible production of the first excited state; and it is only with better spectrometer resolution and also with measurements at larger angles that these two effects can perhaps be separated.

Using the integrated values $C_{XX'}$ of the spectra $S_{XX'}$ we obtained the differential quasielastic cross sections, $[\gamma_{XX'}(\mathrm{d}\sigma/\mathrm{d}\bar{t})_{XX'}]$, up to a factor $\gamma_{XX'}$, for each configuration (X, X') where $\bar{t}$ is the mean value of the momentum transfer t of the scattered α for this partial spectrum. The value of the parameter $\gamma_{XX'}$ has still to be determined.

In fig. 3 the determined values of $[\gamma_{XX'}(\mathrm{d}\sigma/\mathrm{d}\bar{t})_{XX'}]$ are presented, which correspond respectively to α-scattering on a nucleon, a deuteron or a ^{3}He/^{3}H cluster in

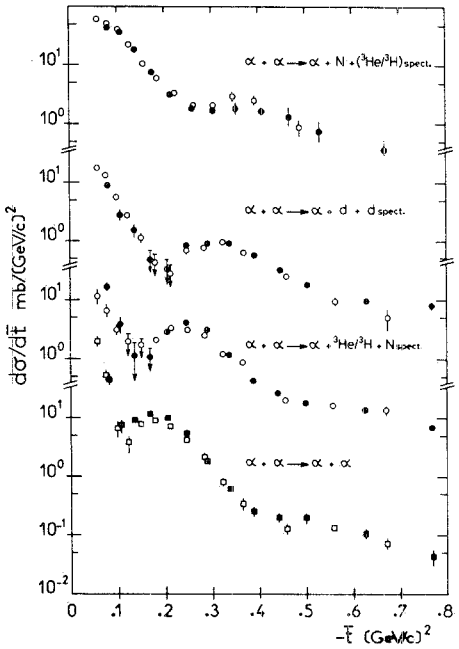

Fig. 3. Partial quasielastic differential cross sections $d\sigma/d\bar{t}$ at 4.32 GeV/c ○ and at 5.07 GeV/c ● obtained by the analysis discussed in the text, along with the $\alpha\alpha$ elastic cross sections for the same incident momenta □ and ■.

the α target, as well as the values of $d\sigma/dt$ previously determined for $\alpha\alpha$ elastic scattering [1]). For the αN quasielastic scattering we have not shown points beyond 9°, since the experimental spectra become too incomplete beyond that angle. The errors shown are uniquely those that result from adjusting the sum of the elementary contributions to the measured spectra. It should be noted that in this figure the value of $\gamma d\sigma/d\bar{t}$ was divided by two in the case of the deuterons so as to account for the existence of two deuterons in the (d, d) configuration of ^{4}He. These data do not show any dependence on the incident energy of the α-particle. On the other hand, in all cases, we observe a diffractive structure whose minima are situated at $t \simeq -0.28$ (GeV/c)^2, -0.20 (GeV/c)^2 and -0.15 (GeV/c)^2 for αN, αd and α-^{3}He/^{3}H quasielastic scattering, respectively, and at -0.11 (GeV/c)^2 for $\alpha\alpha$ elastic scattering. These diffractive structures are characteristic of elastic scattering reactions between light nuclei at these energies.

6. Interpretation of the quasielastic spectra using the glauber theory

6.1. METHOD USED

In order to interpret the quasielastic differential cross sections, $[\gamma d\sigma/d\bar{t}]$, determined in the analysis described in subsect. 5.2, we compare them to the

corresponding cross sections for elastic scattering, taking into account the effect due to the binding energy of the substructures within the target α-particle. This effect is most obvious at low momentum transfers, for $|t|\leq 0.1$ $(\mathrm{GeV}/c)^2$, where the cross section stops increasing exponentially, as can be seen in fig. 3 for the quasielastic differential cross section αN. This low momentum transfer effect has already been observed by Glagolev *et al.* [16]) in the reaction p ^{4}He$\rightarrow$pn with ^{3}He spectator, for pn quasielastic scattering at 1.4 GeV/c.

We have calculated the quasielastic differential cross sections using the Franco and Glauber analysis [31]) originally intended for d-nucleus scattering. According to these authors, the quasielastic cross section can be expressed uniquely as a function of the form factor of the α and the elastic cross sections on the substructures of the α-target; in this case, as is usual in the impulse approximation, double scattering effects are ignored.

(*a*) *The form factor:* to simplify calculations, the wave functions are assumed to be harmonic oscillator wave functions. The α-form factor can be approximated by the gaussian:

$$S(q)=\exp(-q^2\beta^2)\,, \tag{7}$$

q being the transverse momentum ($q\simeq\sqrt{-t}$) and $\beta=R/2\hbar c$, the relation of R to the mean square radius of the nucleus is:

$$R^2=\tfrac{2}{3}\langle\bar{r}^2\rangle\,. \tag{8}$$

For the α-form factor we have used the value $R=1.367$ fm. This corresponds to $\langle\bar{r}^2\rangle^{1/2}=1.674$ fm and is based on the result of Sick *et al.* [32]), which reproduces the Lim function at low transfers [26]).

(*b*) *The elastic cross sections:* due to lack of sufficient experimental data at the energies studied, we have calculated the elastic cross sections αN, αd and α-^{3}He/^{3}H on the basis of the Czyż and Maximon model [33]) which applies the Glauber formalism to nucleus-nucleus collisions. This model has already been used to describe the result of $\alpha\alpha$ elastic scattering cross sections obtained in the same experiment, ref. [1]) and fig. 2. It correctly accounts for the $\alpha\alpha$ elastic scattering data up to the second minimum. This model also provides good fits for αp and αd elastic scattering results in the same energy region and for the same momentum transfers as the present data. This can be seen in fig 4 where the results of Klem *et al.*, for pα elastic scattering [29]) at 560 MeV and those of Aslanides *et al.* [30]) at 650 MeV (respectively, $p=4.64$ and 5.08 GeV/c for the equivalent αp elastic scattering) as well as the results for αd elastic scattering at 3.98 GeV/c [ref. [24–25])] are fitted by the Czyż and Maximon reaction model. It should be remembered that the Czyż and Maximon model is very dependent on nucleon–nucleon interaction parameters, which vary rapidly in our energy domain. The values chosen to describe our results at 4.32 GeV/c and at 5.07 GeV/c are taken from recent experimental results and are those used to describe $\alpha\alpha$ elastic scattering at the same energies [1]). In this model the wave

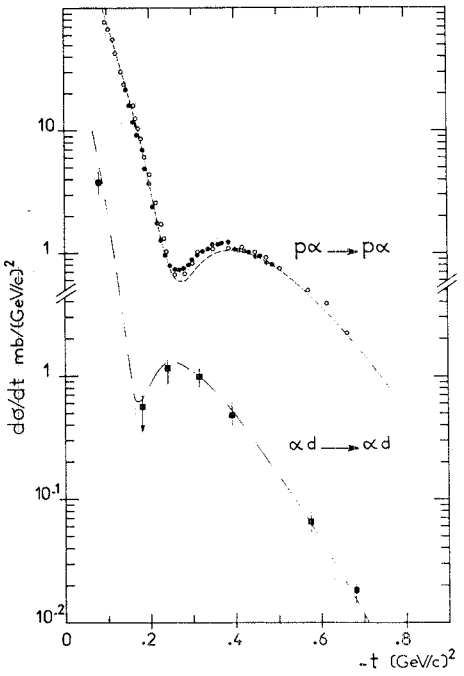

Fig. 4. Differential cross sections for pα elastic scattering at $T_p = 560$ MeV, ○: ref. [29]), and at $T_p = 650$ MeV, ●: ref. [30]), corresponding to αN elastic scattering at P_α equal to 4.64 GeV/c and 5.07 GeV/c, respectively. The dashed curve presents the calculation based on the Czyż and Maximon model with NN parameters at 5.07 GeV/c, as used in ref. [1]) and fig. 2. Differential cross sections for αd elastic scattering at 3.98 GeV/c incident momentum, ■, ref. [24,25]); the dot-dashed curve presents the Czyż and Maximon calculations with $R_d = 1.45$ fm and the NN parameters $\alpha = 0.27$, $\beta = 0.86$ (GeV/c)$^{-2}$, and $\sigma = 30$ mb.

functions are also harmonic oscillator wave functions. They come into the calculation in the form of a nuclear density dependent on the parameter R, already defined:

$$\rho(r) = (\pi/R^2)^{3/2} \exp(-r^2/R^2) . \tag{9}$$

In the case of the αd elastic scattering R_d was adjusted to reproduce the Hulthén function [25]). In this case the relation (8) is not correct since $\langle \bar{r}_d^2 \rangle^{1/2} = 2.28$ fm and $R_d = 1.45$ fm.

6.2. COMPARISON OF THE CALCULATION TO OUR RESULTS

The $d\sigma/d\bar{t}$ cross sections determined from the analysis described in subsect. 5.2 and the results of the calculations are compared in figs 5–7. When the value of R discussed in subsect. 6.1 corresponding to that of the free nucleus is taken for the substructure ^{3}He, ^{3}H or d, it is observed that the position of the diffraction minimum for measured quasielastic cross sections is in the experimental angular distribution at a higher momentum transfer than that of the calculated angular distribution. In order

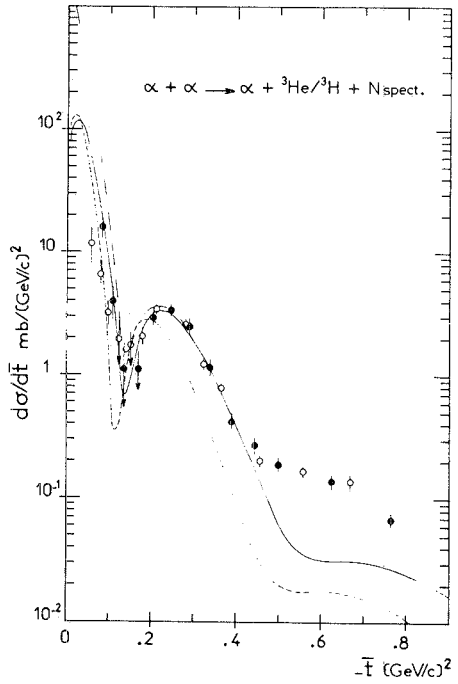

Fig. 5. Comparison of the quasielastic cross sections α-^{3}He/^{3}H with calculations at 5.07 GeV/c based on the Franco and Glauber [31]) and Czyż and Maximon [33]) models. The NN parameters are the same as those used in fig. 2 and ref. [1]). The other parameters used in the calculations are as follows: normalisation factor $\gamma_3 = 0.55$; R_3 (related to the mean square radius of the cluster): dot-dashed line: calculation for the elastic scattering $\alpha - {}^3$He/^{3}H with $R_3 = 1$ fm; solid line: quasielastic scattering with $R_3 = 1$ fm; dashed line: quasielastic scattering with $R_3 = 1.4$ fm, the value-corresponding to that of the free nucleus ^{3}He or ^{3}H. Calculations at 4.32 GeV/c which have a similar behaviour to those at 5.07 GeV/c are not shown.

to correctly reproduce the diffractive behaviour observed, the radius of the substructure within the α was varied in the calculated angular distributions. Within the limit of our errors, these calculations best reproduce the positions of the minimum and the maximum for the experimental angular distributions with the values:

$R_3 = 1 \pm 0.1$ fm for the substructures with 3 nucleons ($\langle r_3^2 \rangle^{1/2} \simeq 1.2$ fm) and

$R_2 = 0.8 \pm 0.1$ fm for the substructures with two nucleons ($\langle \bar{r}_2^2 \rangle^{1/2} \simeq 1$ fm).

To calculate the α binding energy, Sofianos *et al.* [34]) use a distorted wave function for the deuteron of the same radius.

The normalisation factor γ has been deduced from the curves shown in figs 5–7. The ratio of the calculations to the measurements is approximately constant in the region of $-t \leq 0.6$ (GeV/c)^2. For higher momentum transfers where this is no longer true, we have already observed that the Czyż and Maximon model, when applied to our data for $\alpha\alpha$ elastic scattering, predicts a significantly smaller cross section than the values measured. However, it should be noted that double scattering phenomena

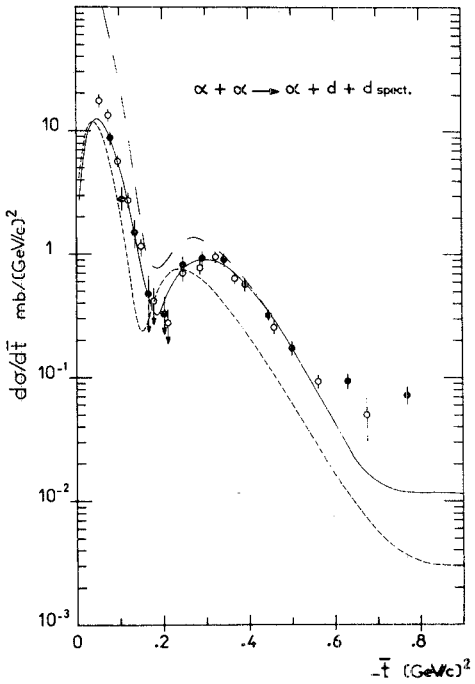

Fig. 6. Comparison between cross sections and calculations similar to that in fig. 5, but for quasielastic αd scattering. The following parameters are used in these calculations: normalisation factor $\gamma_2 = 0.45$; dot-dashed line: elastic scattering with $R_2 = 0.8$ fm; solid line: quasielastic scattering with $R_2 = 0.8$ fm; short dashes: quasielastic scattering with $R_2 = 1.45$ fm, the value corresponding to that of the free deuteron. Calculations at 4.32 GeV/c which have a similar behaviour to those at 5.07 GeV/c are not shown.

can be important at these higher momentum transfers, contributing in a non-negligible way not only to the elastic peak but also to the inelastic spectrum for ^{3}He/^{3}H or d scattering, on the structures (N, ^{3}He/^{3}H) and (d, d). The normalisation factors vary little between 4.32 GeV/c and 5.07 GeV/c. For αd quasielastic scattering $\gamma_2 \simeq 0.45$; and for α-^{3}He/^{3}H, $\gamma_3 \approx 0.55$. These ratios are compatible with the ratio proposed by Bizard and Tekou [17]) for (N, ^{3}He/^{3}H) and with the probability calculated by Lim [21]) for (d, d).

For αN scattering, the normalisation factor γ_1 is close to or somewhat larger than one. This result cannot be explained as resulting solely from scattering on (N, ^{3}He/^{3}H); other contributions must be considered. This excessive cross section can be produced principally by a knock-out reaction on a deuteron or a ^{3}He/^{3}H from the α-target, by interactions in the final state, or even by something like d* production. It can also result from other possible structures of the α: (2N, d) and (4N). From our measurements we cannot exclude the possibility that the contribution attributed to the structure (d, d) is partly due to a (d, 2N) structure which, if it exists, will also contribute to the inelastic spectrum by α-scattering on one of the

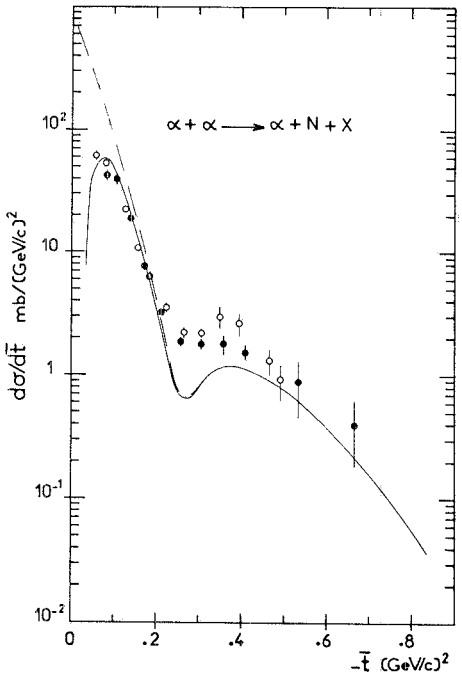

Fig. 7. Comparison between cross sections and calculations similar to that in figs. 5 and 6, but for quasielastic αN scattering. Normalisation factor $\gamma_1 = 1$ dot-dashed line: elastic scattering; solid line: quasielastic scattering. Calculations at 4.32 GeV/c which have a similar behaviour to those at 5.07 GeV/c are not shown.

nucleons, the other nucleon and the deuteron being spectators. We also did an analysis of our results based on the arbitrary supposition that the (d, 2N) contribution was equal to that of the (d, d). This contribution, while it does not change the position of the minima and maxima, does account for the excessive αN cross section observed. However, given the lack of measurements at low momenta, especially at large angles, where the αN spectra with ^{3}He/^{3}H spectator and the αN spectra with (d+N) spectators ought to separate, and in view of the absence of data for (d, 2N) and (4N) structures, we can provide no definite conclusions on the possible role of these structures.

The differential cross section $d\sigma/d^2q$ obtained by adding the quasielastic spectra that describe the interactions α-^{3}He/^{3}H, αd and αN (figs. 5–7) are shown in fig. 2. The diffraction-like structure that we observed around $q = 0.45$ GeV/c is clearly shown.

6.3. CONSISTENCY OF THE PARAMETERS USED IN THIS ANALYSIS

In the interpretation of our experimental data in terms of quasielastic scattering, several parameters have been introduced which are not in fact independent. When

using gaussian wave functions the nuclear radii are linked to the parameter p_0 of the Fermi momentum distribution (form.(6)) by the relation:

$$p_0 = \hbar c/2R\,, \tag{9}$$

which gives $p_0 = 125$ MeV/c for the (d, d) structure a value close to that accepted to describe the quasielastic spectra $(d^2\sigma/d\Omega\, dp)_{lab}$ for αd. Similarly for the ^{3}He/^{3}H substructure $p_0 = 100$ MeV/c, a value for which the Lim distribution [26]) in a gaussian form can easily be fitted.

This same interdependence is equally true of the factors used to normalize the curves calculated in the framework of the Glauber theory with the quasielastic cross sections $d\sigma/d\vec{t}$. In each case a spectroscopic factor can be worked out based on the same radii of the substructures as used in the Glauber calculations, by calculating the overlap wave function. Taking the α wave function to be

$$\phi_4 = \prod_{j=1}^{4} (1/\pi R_\alpha^2)^{3/4} \exp(-r_j^2/2R_\alpha^2)\,, \tag{10}$$

and for ^{3}He/^{3}H

$$\phi_3 = \prod_{i=1}^{3} (1/\pi R_3^2)^{3/4} \exp(-r_i^2/2R_3^2)\,, \tag{11}$$

the overlap wave function is

$$\phi(r_1) = \int \phi_3\phi_4\, d^3r_2\, d^3r_3\, d^3r_4\,, \tag{12}$$

and the spectroscopic factor can be written:

$$\gamma_3 = \int |\phi(r_1)|^2\, d^3r_1 = [2R_\alpha R_3/(R_\alpha^2 + R_3^2)]^9\,. \tag{13}$$

With $R_\alpha = 1.367$ fm and $R_3 = 1$ fm, it is found that $\gamma_3 \simeq 0.6$.

A similar calculation for the 2-nucleon substructure with $R_2 = 0.8$ fm gives:

$$\gamma_2 = [2R_\alpha R_d/(R_\alpha^2 + R_d^2)]^6 \simeq 0.45\,. \tag{14}$$

The spectroscopic factors calculated in this way are thus compatible with the normalisation factors we determined from our experimental data.

7. Conclusion

We have shown that $\alpha + \alpha \rightarrow \alpha + X$ inelastic scattering data can be described as the incoherent sum of the quasielastic scattering of the α-projectile on (N, ^{3}He/^{3}H) and (d, d) structures in the α-target, provided other contributions are included to take into account the excessive αN cross section. The quasielastic scattering cross sections obtained from these data show the same diffractive structure as the corresponding

elastic cross sections. These quasielastic scattering cross sections can be fitted by calculations in the framework of the Glauber formalism provided that radii much inferior to those of the corresponding free nuclei are taken for the 2 and 3 nucleons substructures. *A priori* this is satisfactory since the radii of the free ^{3}He, ^{3}H and d are greater than that of the ^{4}He. The compatibility between the various parameters introduced in this analysis should be stressed: in the gaussian representation of the wave functions used in the present work all of these — probability density, Fermi momentum distribution, and normalisation factor of each substructure — are defined by the same parameter R.

In future measurements with better resolution and a larger range of momentum transfer, it should be possible to determine whether the excitation of excited states in the α contributes significantly to the experimental spectra, to separate the double scattering contribution, and perhaps to explain the behaviour of the αN spectrum. Also, for measurements at higher energies, since the distortions of the wave functions are smaller and the approximations in the Glauber formalism are more valid, the comparison of the experimental measurements with the calculations of quasielastic scattering of the incident on the 2 and 3 nucleon substructures within the α should be more valid. Finally small-angle measurements would allow us to check our analysis in the domain of low momentum transfer and to measure the total quasielastic cross sections.

We acknowledge Dr F. Plouin for an important contribution to this work. We wish to thank Drs M. Chemtob, R. Frascaria, G. V. Giaî, R. J. Glauber, A. S. Goldhaber, J. Hüfner, B. Marini, A. Tékou and C. Whitten, for stimulating discussions. We thank also M. P. Guillouet and M. G. Simonneau for their technical support.

References

1) J. Berger, J. Duflo, L. Goldzahl, J. Oostens, F. Plouin, F.L. Fabbri, P. Picozza, L. Satta, G. Bizard, F. Lefebvres, J.C. Steckmeyer and D. Legrand, Nucl. Phys. **A260** (1980) 421
2) P.G. Roos, Phys. Rev. **C9** (1974) 2437
3) N.S. Chant and P.G. Roos, Phys. Rev. **C15** (1977) 57
4) G. Bizard, C. Le Brun, J. Berger, J. Duflo, L. Goldzahl, F. Plouin, J. Oostens, M. van den Bossche, L. Vu Hai, F.L. Fabbri, P. Picozza and L. Satta, Nucl. Phys. **A285** (1977) 461
5) H. Quéchon, Thesis, University of Orsay, 91400 Orsay (France) (7/1980)
6) R.J. Glauber and G. Matthiae, Nucl. Phys. **B21** (1970) 135
7) T. Fujita and J. Hüfner, Phys. lett. **87B** (1979) 327
8) J. Duflo, J. Berger, L. Goldzahl, J. Oostens, F. Plouin, F.L. Fabbri, P. Picozza, L. Satta, G. Bizard, F. Lefebvres and J.C. Steckmeyer, in Abstract Volume of Contributed Papers, 8th Int. Conf. on high energy physics and nuclear structure, Vancouver (1979) ed. TRIUMF, University of British Columbia Vancouver, British Columbia V6T IW5, Canada
9) H. Palevsky, J. L. Friedes, R.J. Sutter, G.W. Bennett, G.J. Igo, W.D. Simpson, G.C. Phillips, D.M. Corley, N.S. Wall, R.L. Stearns and B. Gottschalk, Phys. Rev. Lett. **18** (1967) 1200
10) J. Hüfner, private communication (1980)

11) E.E. Gross, E.V. Hungerford III, J.J. Malanify, H.G. Pugh and J.W. Watson, Phys. Rev. **178** (1969) 1584
12) E.L. Haase, W.N. Wang and M.A. Fawzi, Nucl. Phys. **A178** (1971) 81
13) J.J. Bevelacqua, Phys. Rev. **C19** (1979) 2050
14) N. Frascaria, C. Stéphan, P. Colombani, J.P. Garron, J.C. Jacmart, M. Riou and L. Tassan-Got, Phys. Rev. Lett. **39** (1977) 913
15) K.F. Liu and G.E. Brown, Nucl. Phys. **A265** (1976) 385
16) V.V. Glagolev, R.M. Lebedev, I.S. Saitov, V.N. Streltsov, L.I. Zuravleva, A.N. Gorbunov, K.U. Khayretdinov, G. Martinska, I. Patočka, M. Seman, H. Braun, A. Fridman, J.P. Gerber, H. Johnstad, P. Juillot, A. Michalon, B.S. Aladashvili, M.S. Nioradze, T. Siemiorczuk, T. Sobczak, J. Stepaniak and P. Zielinski, Phys. Rev. **C18** (1978) 1382
17) G. Bizard and A. Tekou, Clustering aspects of nuclear structure and nuclear reactions (Winnipeg, 1978), AIP Conf. Proc. No. 47 (1978) p. 620; Nuovo Cim. **51A** (1979) 114
18) J. R. Wu, C. C. Chang and H.D. Holmgren, Phys. Rev. lett. **40** (1978) 1013
19) R. Serber, Phys. Rev. **72** (1947) 1008
20) R. Frascaria, P.G. Roos, M. Morlet, N. Marty, A. Willis, V. Comparat and N. Fujiwara, Phys. Rev. **C12** (1975) 243
21) T.K. Lim, Phys. Rev. **C14** (1976) 1243
22) E.F. Redish, G.J. Stephenson, Jr. and G.M. Lerner, Phys. Rev. **C2** (1970) 1665
23) L.S. Azhgivey, M.A. Ignatenko, V.V. Ivanov, A.S. Kuznetsov, M.G. Mescheryakov, S.V. Razin, G.D. Stoletov, A.V. Tarasov, V.V. Uzhinsky, I.K. Vzorov and V.N. Zhmyrov, Nucl. Phys. **A305** (1978) 397
24) J. Berger *et al.*, to be published
25) B. Marini, Thèse de 3ème cycle, Université de Caen, 14000 Caen (France) (1979)
26) T.K. Lim, Phys. Lett. **44B** (1973) 341
27) A.S. Goldhaber, Phys. Lett. **53B** (1974) 306
28) J.R. Wu, C.C. Chang, H.D. Holmgren and R.W. Koontz, Phys. Rev. **C20** (1979) 1284
29) R. Klem, G. J. Igo, R. Talaga, A. Wreikat, H. Courant, K. Einsweiler, J. Joyce, H. Kagan, Y.I. Makdisi, M.L. Marshak, B. Mossberg, E.A. Peterson, K. Ruddick and T. Walsh, Phys. Rev. Lett. **38** (1977) 1272
30) E. Aslanides, T. Bauer, R. Bertini, R. Beurtey, A. Boudard, F. Brochard, G. Bruge, A. Chaumeaux, H. Catz, J.M. Fontaine, R. Frascaria, D. Garreta, P. Gorodetzky, J. Guyot, F. Hibou, D. Legrand, M. Matoba, Y. Terrien, J. Thirion and E. Lambert, Phys. Lett. **68B** (1977) 221
31) V. Franco and R.J. Glauber, Phys. Rev. **142** (1966) 1195
32) J.S. McCarthy, I. Sick and R.R. Whitney, Phys. Rev. **C15** (1977) 1396
33) W. Czyż and L.C. Maximon, Ann. of Phys. **52** (1962) 59
34) S. Sofianos, H. Fiedeldey and N.J. McGurk, Phys. lett. **68B** (1977) 117